Video Article

Development of an Experimental Setup for the Measurement of the Coefficient of Restitution under Vacuum Conditions

Sven Drücker[1], Isabell Krautstrunk[2], Maria Paulick[2], Khashayar Saleh[1], Martin Morgeneyer[1], Arno Kwade[2]

[1]Industrial Process Engineering, University of Technology of Compiègne

[2]Institute for Particle Technology, Technische Universität Braunschweig

Correspondence to: Sven Drücker at sven.druecker@tuhh.de

URL: https://www.jove.com/video/53299
DOI: doi:10.3791/53299

Keywords: Engineering, Issue 109, Restitution coefficient, impact and rebound velocity, free-fall experiment, vacuum, micrometer particles, high-speed camera

Date Published: 3/29/2016

Citation: Drücker, S., Krautstrunk, I., Paulick, M., Saleh, K., Morgeneyer, M., Kwade, A. Development of an Experimental Setup for the Measurement of the Coefficient of Restitution under Vacuum Conditions. *J. Vis. Exp.* (109), e53299, doi:10.3791/53299 (2016).

Abstract

The Discrete Element Method is used for the simulation of particulate systems to describe and analyze them, to predict and afterwards optimize their behavior for single stages of a process or even an entire process. For the simulation with occurring particle-particle and particle-wall contacts, the value of the coefficient of restitution is required. It can be determined experimentally. The coefficient of restitution depends on several parameters like the impact velocity. Especially for fine particles the impact velocity depends on the air pressure and under atmospheric pressure high impact velocities cannot be reached. For this, a new experimental setup for free-fall tests under vacuum conditions is developed. The coefficient of restitution is determined with the impact and rebound velocity which are detected by a high-speed camera. To not hinder the view, the vacuum chamber is made of glass. Also a new release mechanism to drop one single particle under vacuum conditions is constructed. Due to that, all properties of the particle can be characterized beforehand.

Video Link

The video component of this article can be found at https://www.jove.com/video/53299/

Introduction

Powders and granules are everywhere around us. A life without them is impossible in modern societies. They appear in food and drinks as grains or even flour, sugar, coffee and cocoa. They are needed for daily used objects like the toner for laser printer. Also the plastic industry is not imaginable without them, because plastic is transported in granular form before it is melted and given a new shape. After Ennis *et al.*[1] at least 40% of the value added to the consumer price index of the United States of America by the chemical industry (agriculture, food, pharmaceuticals, minerals, munitions) is connected to particle technology. Nedderman[2] even stated that about 50% (weight) of the products and a minimum of 75% of the raw materials are granular solids in the chemical industry. He also declared that there occur many problems concerning storage and transportation of granular materials. One of these is that during transport and handling many collisions take place. To analyze, describe and predict the behavior of a particulate system, Discrete Element Method (DEM) simulations can be performed. For these simulations knowledge of the collision behavior of the particulate system is necessary. The parameter that describes this behavior in DEM simulations is the coefficient of restitution (COR) that has to be determined in experiments.

The COR is a number that characterizes the loss of kinetic energy during the impact as described by Seifried *et al.*[3]. They explained that this is caused by plastic deformations, wave propagation and viscoelastic phenomena. Thornton and Ning[4] also mentioned that some energy might be dissipated by work due to interface adhesion. The COR depends on impact velocity, material behavior, particle size, shape, roughness, moisture content, adhesion properties and temperature as stated in Antonyuk *et al.*[5]. For a completely elastic impact all absorbed energy is returned after the collision so that the relative velocity between the contact partners is equal before and after the impact. This leads to a COR of $e = 1$. During a perfectly plastic impact all the initial kinetic energy is absorbed and the contact partners stick together which leads to a COR of $e = 0$. Furthermore, Güttler *et al.*[6] explained that there are two types of collisions. On the one hand, there is the collision between two spheres which is also known as the particle-particle contact. On the other hand, there is the collision between a sphere and a plate that is also called particle-wall contact. With the data for the COR and other material properties like coefficient of friction, density, Poisson's ratio and shear modulus DEM simulations can be performed to determine the post-collisional velocities and orientations of the particles as explained by Bharadwaj *et al.*[7]. As shown in Antonyuk *et al.*[5], the COR can be calculated with the ratio of rebound velocity to impact velocity.

Therefore an experimental setup for free-fall tests to examine the particle-wall contact of particles with a diameter from 0.1 mm to 4 mm was constructed. The advantage of free-fall experiments compared to accelerated experiments as in Fu *et al.*[8] and Sommerfeld and Huber[9] is that rotation might be eliminated. Hence, the transfer between rotational and translational kinetic energy which influences the COR can be avoided. Aspheric particles need to be marked as in Foerster *et al.*[10] or Lorenz *et al.*[11] to take rotation into account. As the COR is depending on the impact velocity, the impact velocities in the experiments have to match the ones in the real transport and handling processes. In free-fall experiments under atmospheric pressure, the impact velocity is limited by the drag force, having an increasing influence for a decreasing particle

size. To overcome this drawback, the experimental setup works under vacuum conditions. A second challenge is to drop just one single particle since then it is possible to characterize all properties that influence the COR beforehand, for instance surface roughness and adhesion. With this knowledge, the COR can be determined according to the properties of the particle. For this, a new release mechanism was developed. Another issue is the adhesive forces of powders with a diameter inferior to 400 µm. Therefore, a dry and ambient temperature environment is necessary to overcome adhesion.

The experimental setup consists of several parts. An exterior view of the existing experimental setup is shown in **Figure 1**. First, there is the vacuum chamber that is made out of glass. It is composed of a lower part (cylinder), a top cover, a seal ring and a sleeve to connect the parts. The lower part has two openings for a connection with the vacuum pump and the vacuum gauge. The top cover has four openings. Two of them are necessary for the sticks of the release mechanism described below and also two that can be used for further improvements of the experiment. All these openings can be closed with seal rings and screw caps when working under vacuum conditions.

Moreover, a new release mechanism was developed since the use of a vacuum nozzle as in many other experiments documented in literature (for example Foerster *et al.*[10], Lorenz *et al.*[11], Fu *et al.*[12] or Wong *et al.*[13]) is not possible in a vacuum environment. The mechanism is realized by a cylindrical chamber with a conical drill hole that is held by a plate. This is connected to a stick that fits in one of the seal rings of the top cover of the vacuum chamber and guarantees the adjustment of a variable initial height for the free-fall experiments. A scale is drawn on the stick for measuring the height. The closing of the particle chamber is implemented by a conical tip of a pipette that is again connected to a stick. The new release mechanism can be seen in **Figure 2** and works as described here: in the initial state the pipette tip is pushed down so that the circumference of the tip touches the edge of the chamber's drill hole. The chamber is closed with the pipette tip such that there is no space for a particle to leave the chamber through the hole. To release the particle, the stick is pulled upwards very slowly together with the tip connected to it. As the diameter of the tip is getting smaller a gap between its circumference and the edge of the drill hole arises through which the particle can leave the chamber. Although one might expect a rotation of the particle with the newly developed release mechanism as the particle could 'roll' out of the chamber, a different behavior appears in the experiments. **Figure 3** shows the impact of an aspherical particle from 50 frames before to 50 frames after the impact in steps of 25 frames. From the shape of the particle no rotation is visible before the impact (1-3) whereas afterwards it obviously spins (4-5). Therefore the claimed non-rotational release is taking place with this release mechanism.

Another component of the experimental setup is the baseplate. In fact there are three different kinds of baseplates consisting of different materials. One is made of stainless steel, a second of aluminum and a third of polyvinyl chloride (PVC). These baseplates represent frequently used materials in process engineering for example in reactors and tubes.

To determine the impact and rebound velocities, a high-speed camera with 10,000 fps and a resolution of 528 x 396 pixels is used. This configuration is chosen as there is always one picture near the impact and also the resolution is still satisfactory. The camera is connected to a screen that shows the videos in the instant when they are recorded. This is necessary, because the high speed camera can only save a limited amount of pictures and overwrites the beginning of the video when this amount is exceeded. Furthermore, a strong light source for the illumination of the visual field of the high-speed camera is required. For illumination uniformity a sheet of technical drawing paper is glued on the backside of the vacuum chamber that spreads the light.

Finally, a two-stage rotary vane pump is used to establish a vacuum of 0.1 mbar and a vacuum gauge measures the vacuum to guarantee constant environmental conditions.

For the here presented work glass beads with different particle diameters (0.1-0.2, 0.2-0.3, 0.3-0.4, 0.700, 1.588, 2.381, 2.780, 3.680 and 4.000 mm) are used. The beads are made of soda lime glass and are spherical with a rather smooth surface.

Protocol

1. Experiments with Particles Coarser or Equal to 700 µm

1. Preparation of the experimental setup
    1. Remove the sleeve and lift the top cover of the vacuum chamber. Place the baseplate consisting of the desired wall material in the vacuum chamber. Turn the lower part of the vacuum chamber sideways to slide in the plate carefully by hands.
    2. Place exactly one of the particles to be examined with tweezers in the center of the baseplate. Afterwards adjust the height of the camera with a tripod in such a way that the baseplate is in the lowest quarter of the visual field and focus on the particle.
    3. Remove the particle using tweezers.

2. Experimental Procedure
    1. Adjust the height of the particle chamber in such a way that the desired impact velocity of the particle is reached. Use the scale on the stick attached to the holding plate as an indicator of the height. Close the particle chamber with the tip of the pipette by pushing it down so that the circumference of the pipette touches the edge of the chamber's drill hole. Open the sleeve and lift the top cover of the vacuum chamber.
    2. Put one single sphere in the particle chamber with tweezers. The sphere can be solid or liquid-filled (as in Louge *et al.*[14]), depending on what kind of particles shall be analyzed. However, in this work only solid particles are examined. Place the top cover on the lower part of the vacuum chamber (cylinder) and connect the top cover and the lower part of the vacuum chamber with the sleeve.
    3. Evacuate the chamber with the vacuum pump until a level of 0.1 mbar (or any other desired value) is reached. Measure the pressure with a vacuum gauge. Close the valve at the side of the vacuum chamber and turn off the vacuum pump. Wear safety goggles when working under vacuum conditions.
    4. Apply a frame rate of 10,000 fps and adjust the camera settings (position/zoom) to obtain a resolution of 528 x 396 pixels. Start the recording of the high-speed camera and open the hole of the particle chamber to liberate the particle. Simultaneously pull and turn the stick attached to the tip of the pipette to avoid stick-slip problems due to high friction between stick and seal ring.

5. Stop the recording of the camera directly after impact because only a limited amount of pictures can be saved and the first ones are overwritten when this limit is exceeded. Cut the movie around the instant of the impact at the screen and save it on the memory card.
6. Repeat the experiment ten times to obtain statistically significant results. The results are statistically significant if after ten repetitions, the mean value does not alter anymore (this might be different for other materials depending on the homogeneity of the sample or other particle shapes).

3. Evaluation Procedure
    1. Calibrate the software with the known size of a particle or another object using one frame of the video made in step 1.2.4 to obtain a conversion between pixels and distances. Use the horizontal diameter as it is not blurred due to the particle's motion.
        1. Count the number of pixels of the horizontal diameter and then divide the known distance by the number of pixels to get the conversion factor 'distance per pixel'. A picture of the calibration process is shown in **Figure 4**.
    2. Set a reference point of motion on the top of the sphere ten frames before and one frame before the impact to calculate the impact velocity. **Figure 5** presents the two reference points of motion. With the conversion factor from step 1.3.1, use the number of pixels between the two points to obtain the travelled distance. Divide the distance by the passed time (product of number of frames and time step) to obtain the impact velocity.
    3. Set a reference point of motion on the top of the sphere one frame after and ten frames after the impact to calculate the rebound velocity. Determine the rebound velocity analogously to step 1.3.2.
    4. Calculate the COR as ratio of rebound velocity to impact velocity.
    5. Repeat the steps 1.3.1-1.3.4 for the evaluation of all recorded drop test videos.

2. Experiments with Powders Finer or Equal to 400 µm

1. Preparation of the experimental setup
    1. Remove the sleeve and lift the top cover of the vacuum chamber. Place the baseplate consisting of the desired wall material in the vacuum chamber. Turn the lower part of the vacuum chamber sideways to slide in the plate carefully by hands.
    2. Place an adequate reference object such as a particle with a known size in the center of the baseplate with tweezers. Afterwards adjust the height of the camera with a tripod in such a way that the baseplate is in the lowest quarter of the visual field and focus the reference object.
    3. Record a short video of the reference object when it is lying on the baseplate with exactly the same settings as in the following experiments.
    4. Remove the reference object using tweezers.

2. Experimental Procedure
    1. Adjust the height of the particle chamber in such a way that the desired impact velocity of the particle is reached. Use the scale on the stick attached to the holding plate as an indicator of the height. Close the particle chamber with the tip of the pipette by pushing it down so that the circumference of the pipette touches the edge of the chamber's drill hole. Open the sleeve and lift the top cover of the vacuum chamber.
    2. Put 50 to 100 spheres in the particle chamber. To guide the spheres into the particle chamber, deposit them first on a folded sheet of paper. Use the folded paper as a groove to slide the particles into the chamber. Place the top cover on the lower part of the vacuum chamber (cylinder) and connect the top cover and the lower part of the vacuum chamber with the sleeve.
    3. Evacuate the chamber with the vacuum pump until a level of 0.1 mbar (or any other desired value) is reached. Measure the pressure with a vacuum gauge. Close the valve at the side of the vacuum chamber and turn off the vacuum pump. Wear safety goggles when working under vacuum conditions.
    4. Start the recording of the high-speed camera with 10,000 fps and a resolution of 528 x 396 pixels and open the hole of the particle chamber to liberate the particles. Simultaneously pull and turn the stick attached to the tip of the pipette to avoid stick-slip problems due to the high friction between stick and seal ring. Pull very slowly to prevent that all the particles drop at the same time.
    5. Stop the recording of the camera 5 to 6 sec after the impact of the first particle because only a limited amount of pictures can be saved and the first ones are overwritten when this limit is exceeded. Cut the movie at the screen in such a way that at least 10 clearly focused impacts of particles are visible and save it on the memory card.

3. Evaluation Procedure
    1. Calibrate the software with the known size of the reference object from the video of step 2.1.3 to obtain a conversion between pixels and distances. Count the number of pixels of the size of the reference object and then divide the known distance by the number of pixels to get the conversion factor 'distance per pixel'.
    2. Set a reference point of motion on the top of the first clearly focused sphere in the video ten frames before and one frame before the impact to calculate the impact velocity. Calculate the impact velocity analogously to step 1.3.2 together with the conversion factor from step 2.3.1.
    3. Set a reference point of motion on the top of the first clearly focused sphere one frame after and ten frames after the impact to calculate the rebound velocity. Calculate the rebound velocity analogously to step 2.3.2.
    4. Calculate the COR as ratio of rebound velocity to impact velocity.
    5. Repeat steps 2.3.2-2.3.3 for the evaluation of the impacts of another nine clearly focused spheres.

Representative Results

For the analysis glass particles with a diameter of 100 µm to 4.0 mm were dropped from an initial height of 200 mm on a stainless steel baseplate with a thickness of 20 mm.

Figure 6 shows the mean values as well as the maximum and minimum values for the COR depending on the particle size for atmospheric pressure and vacuum. The mean value of the COR is found to be approximately e = 0.9 for particles greater or equal to 700 µm independent of the air pressure.

For particles with a diameter less than 400 µm the COR stays nearly constant with a value of e = 0.9 under vacuum conditions. Under atmospheric pressure the COR decreases with decreasing particle diameter. A reason for this could be that the air in front of the particle is compressed during the free-fall which results in kind of a cushion that damps the collision, absorbs kinetic energy and due to that leads to a lower COR. In both cases the deviations are higher than for coarser particles. An explanation for this might be that the fine particles only had the size of a few pixels in the videos. Therefore the error due to the choice of the pixels in a blurred picture is intense.

The results for the impact velocity depending on the particle size for atmospheric pressure and vacuum are presented in **Figure 7**. For the impact velocity the mean values, the maximum and the minimum are shown. The mean value of the impact velocity is evaluated with approximately v_i = 2 $msec^{-1}$ for particles greater than 700 µm independent of the air pressure. An exception appears for a particle diameter of 700 µm where the impact velocity is significantly lower under vacuum conditions and even slightly more under atmospheric pressure. For a decreasing particle diameter a decreasing impact velocity under atmospheric pressure was expected. In contrast to that, the impact velocity should stay the same under vacuum conditions. Having a closer look at the evaluation method it can be seen that for the particles with a diameter of 700 µm the calibration for the conversion between pixels and distances is different to that for the coarser particles. The ratio of pixels per millimeter is significantly higher which results in lower velocities. A reason for the false calibration might be that the camera is not able to correctly recognize the shape of the finer particles. Using the same standardized calibration as for the coarser particles the impact velocities are still approximately in the same range and the outliers can be eliminated.

For powders with a diameter inferior to 400 µm the impact velocity decreases significantly with a decreasing particle diameter under atmospheric pressure. The equilibrium of air friction force and gravitational force, and also the settling velocity, is reached earlier for finer particles. In contrast to that, the impact velocity under vacuum conditions is nearly constant also for the powders. This proves the theory of an infinitely accelerating particle, when there is no air that can result in a drag force and because of that an equilibrium of forces is never reached. It also shows the necessity of vacuum conditions and therefore also the newly developed release mechanism to reach high impact velocities with fine particles. In these experiments just a slight decrease of the impact velocity is recognizable that can be explained by the fact that only a vacuum of 0.1 mbar was reached which is not a perfect vacuum. The much higher deviations for particles with a median diameter of 0.113 mm occur as the influence of the error due to the choice of the pixels in a blurred picture is higher for lower velocities.

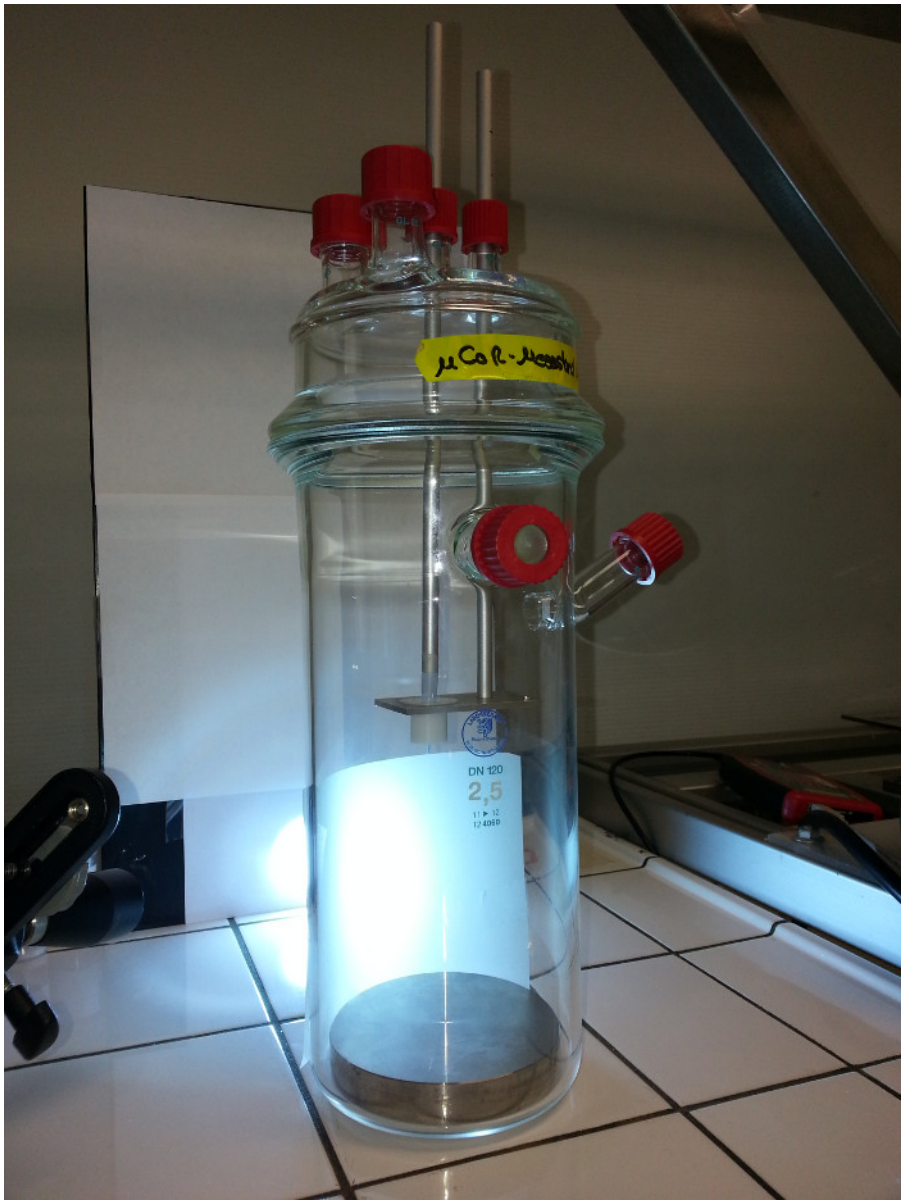

Figure 1. Exterior view of the vacuum chamber. This figure shows the vacuum chamber from the side. One can see the lower part with its two openings for a connection with the vacuum pump and the vacuum gauge. Moreover, the top cover with four openings with seal rings and screw caps are visible. The seal ring is between the lower part and the upper part. The sleeve was removed in this picture. Please click here to view a larger version of this figure.

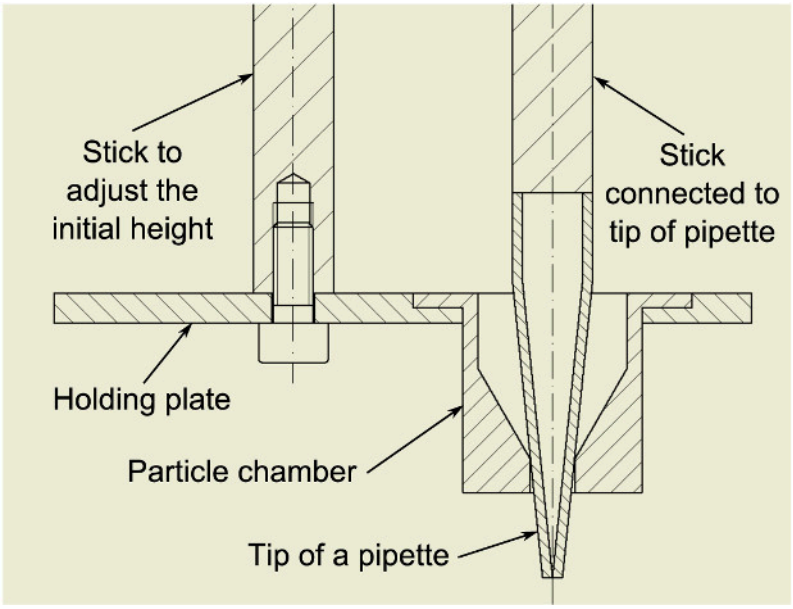

Figure 2. Release mechanism with particle chamber and tip of a pipette. This figure describes the newly developed release mechanism for vacuum experiments. Firstly, the plate holding the cylindrical chamber with a conical drill hole can be seen. In addition, the two sticks for the adjustment of a variable initial height and the connection to the conical tip of a pipette are presented. Please click here to view a larger version of this figure.

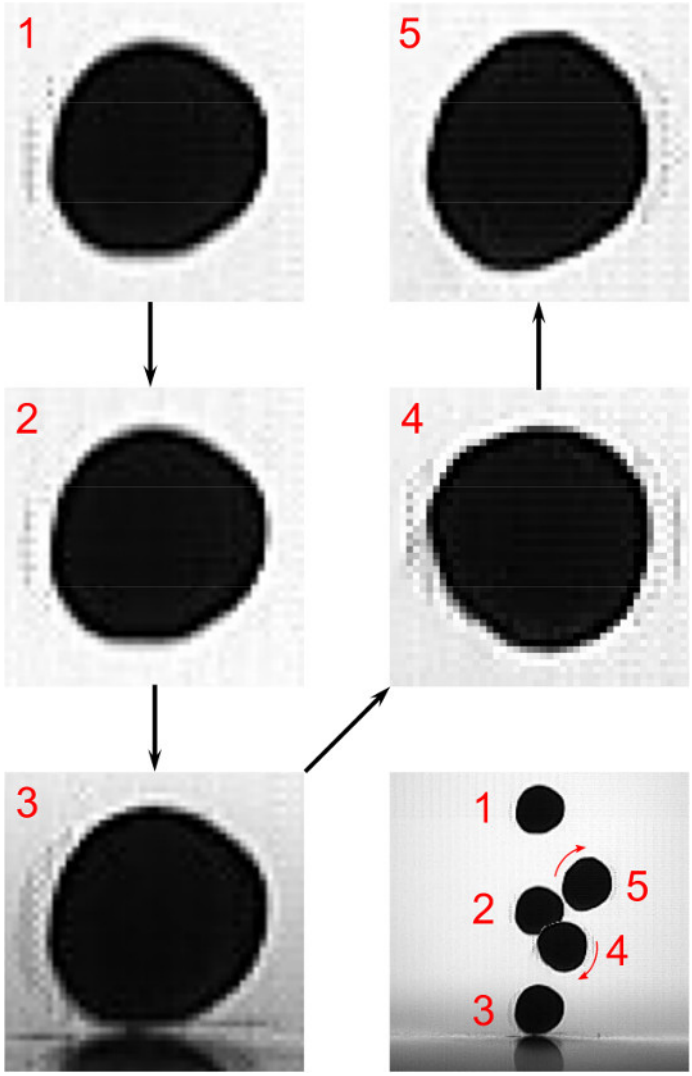

Figure 3. Non-rotational release. This figure shows a series of pictures of an aspherical particle from 50 (1) and 25 frames (2) before the impact as well as at the impact (3) and at 25 (4) and 50 (5) frames after the impact. The identical shape of the particle up to the impact reveals the non-rotational release. Please click here to view a larger version of this figure.

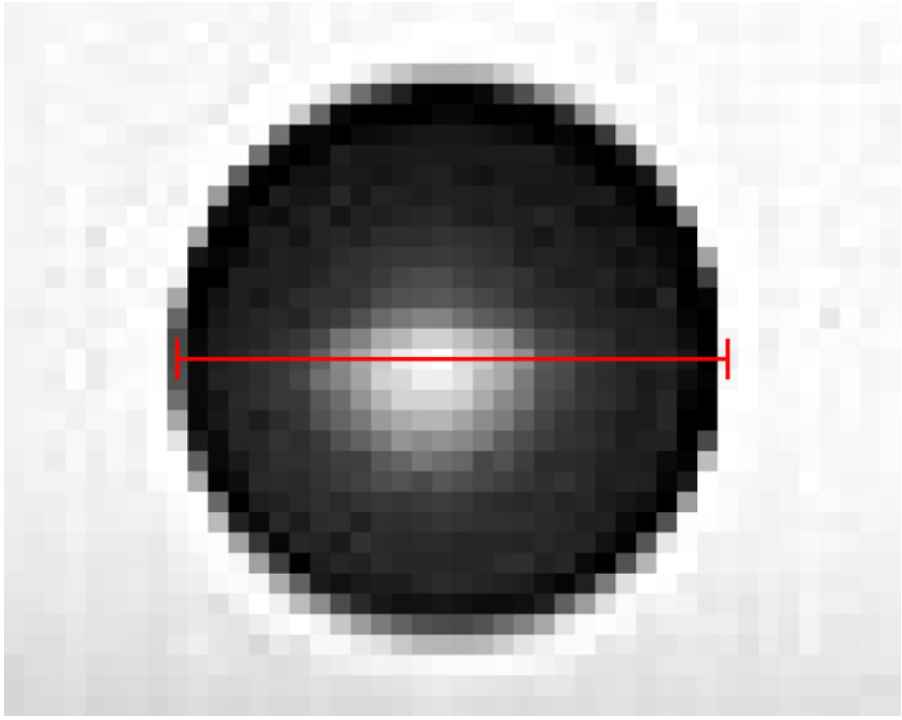

Figure 4. Calibration of the software. This figure shows a particle from a video of a recorded free-fall experiment. The red line represents the size of the particle and embraces the number of pixels necessary for calculating the conversion factor. Please click here to view a larger version of this figure.

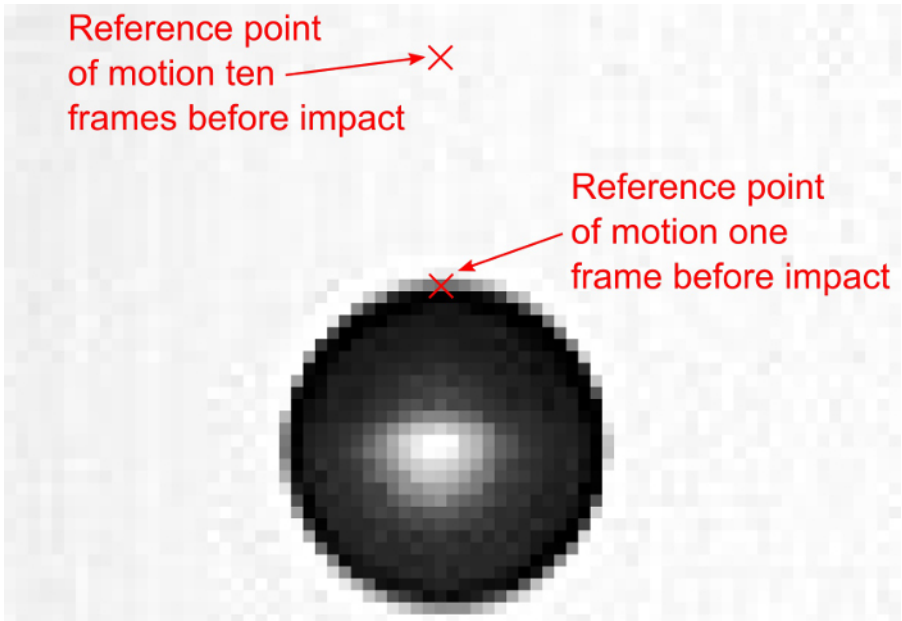

Figure 5. Reference point of motion. This figure presents a particle in a video of a recorded free-fall experiment. The two red crosses illustrate the two reference points of motion on the top of the sphere in the respective frame: the upper one at ten frames before the impact and the lower one at one frame prior to the impact. The distance between the two points is used to calculate the impact velocity of the particle. Please click here to view a larger version of this figure.

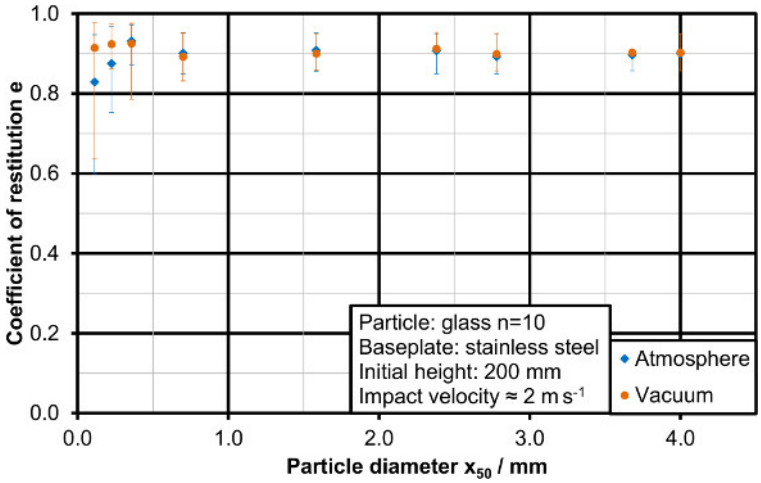

Figure 6. Influence of particle size and air pressure on the COR. This figure shows the mean values as well as the maximum and minimum values with the error bars for the COR depending on the particle size. The blue diamonds represent results for experiments under atmospheric pressure whereas the orange circles show results for experiments under vacuum conditions. Glass particles were dropped on a stainless steel baseplate from an initial height of 200 mm. Each data point represents the mean value of ten repetitions of the experiment. Please click here to view a larger version of this figure.

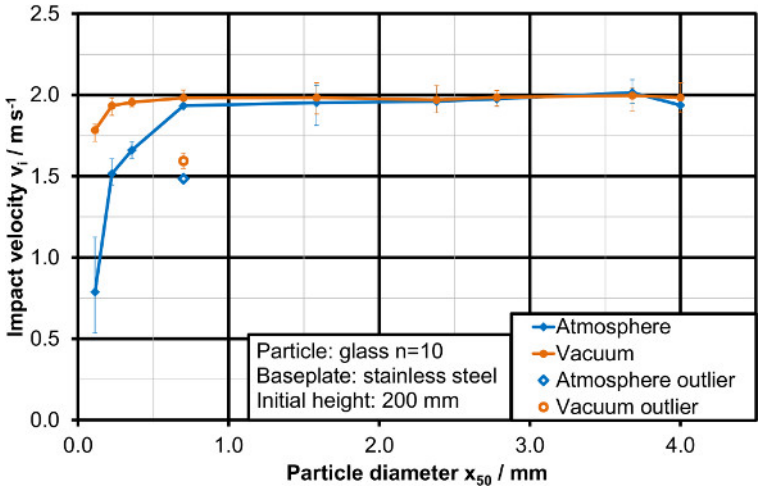

Figure 7. Influence of particle size and air pressure on the impact velocity. This figure shows the mean values for the impact velocity depending on the particle size. Moreover the maximum and minimum values depicted by the error bars are presented. The filled blue diamonds demonstrate results for experiments under atmospheric pressure whereas the filled orange circles display results for experiments under vacuum conditions. The empty diamond and the empty circle illustrate outliers because of calibration issues. In the experiments glass particles were dropped on a stainless steel baseplate from an initial height of 200 mm. Each data point represents the mean value of ten repetitions of the experiment. Please click here to view a larger version of this figure.

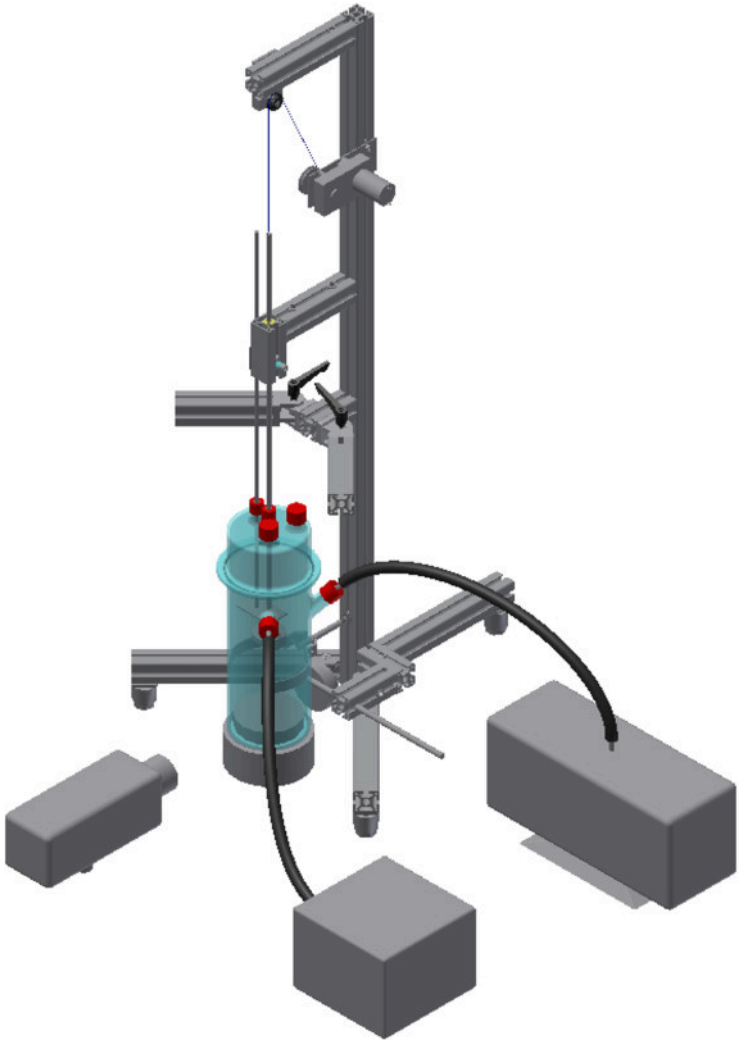

Figure 8. The future experimental setup. This figure depicts the future experimental setup to minimize the instability of the particle chamber during the release. The automated setup with the stick guided by bushings, as well as the wire for the connection of the stick to the motor via two pulleys is shown. Also the frame is displayed. Please click here to view a larger version of this figure.

Discussion

To validate the functionality of the experimental setup in general, tests with similar material combinations as in other established setups (Antonyuk *et al.*[5] and Wong *et al.*[13]) were performed. Since very similar results were obtained, the general procedure seems to work. Nevertheless, caution has to be taken towards the procedure and the analysis and further improvements are necessary.

The main limitation of the experimental setup is the quality of the videos. On the one hand, the images can be blurred because the particle is not exactly in the visual field of the camera. Here, the particle impacts not perfectly centric due to instability of the particle chamber during particle release. On the other hand, the resolution is responsible for the accuracy of determining the velocities, because the number of pixels limits the number of nuances. Therefore it is necessary to test different frame rates since the higher the frame rate the lower the resolution. To avoid calibration problems of the conversion between pixels and distances as in the experiments with 700 µm particles, a standardized calibration with a video of a reference object with an adequate, known size should be taken with exactly the same camera settings as in the experiments. A recommendation for such an object could be a ruler placed at the impact position of the particle. This object would also be preferable for experiments with larger particles since larger reference distances reduce the calibration error.

To minimize the instability of the particle chamber during the release, the setup will be automated and the stick connected to the tip of the pipette will be guided by bushings. A wire is connected to the top of the stick and then guided over one pulley aligned above the stick to another pulley connected to a motor that pulls the wire. Therefore also a frame is constructed. The future setup is shown in **Figure 8**.

To be able to release powders inferior to 20 µm several improvements will be made. For these fine particles adhesive forces much higher than the gravitational ones occur so that particles stick together and to walls. Therefore a vibration of the particle chamber and the needle could be a means to overcome the adhesive forces and make the particle leave the chamber. Another difficulty is that these particles are too small to be visible during the experiment. Therefore a sensor is required that indicates the instant when the particle falls because the high speed camera can

only save a limited amount of pictures and overwrites the beginning of the video when this is exceeded. Moreover, a microscope objective will be mounted on the camera to be able to analyze particles down to 10 µm.

Also the particle-particle contact needs to be examined to be able to characterize all collisions in DEM simulation. One possibility to evaluate this could be to place many particles on the baseplate and to carry out the drop experiment for an impact on a particle then. Another idea to analyze the particle-particle contact would be to modify this experimental setup and apply a similar technique to the one of Foerster *et al.*[10] and Lorenz *et al.*[11]. In their experiments two particles were liberated with different initial heights and collide before the impact on the ground. Afterwards the results for the particle-particle and the particle-wall contact need to be compared.

Disclosures

The authors have nothing to disclose.

Acknowledgements

The authors have no acknowledgements.

References

1. Ennis, B.J., Green, J., Davies, R. The legacy of neglect in the U.S. *Chem. Eng. Prog.* **90** (4), 32-43 (1994).
2. Nedderman, R.M. *Statics and Kinematics of Granular Materials.* Cambridge: Cambridge University Press, (1992).
3. Seifried, R., Schiehlen, W., Eberhard, P. Numerical and experimental evaluation of the coefficient of restitution for repeated impacts. *Int. J. Impact Eng.* **32**, 508-524 (2005).
4. Thornton, C., Ning, Z. A theoretical model for the stick/bounce behaviour of adhesive, elastic-plastic spheres. *Powder Technol.* **99**, 154-162 (1998).
5. Antonyuk, S., *et al.* Energy absorption during compression and impact of dry elastic-plastic spherical granules. *Granul. Matter.* **12**, 15-47 (2010).
6. Güttler, C., Heißelmann, D., Blum, J., Krijt, S. Normal Collisions of Spheres: A Literature Survey on Available Experiments. *arXIV.* arXiv:1204.0001 (2012).
7. Bharadwaj, R., Smith, C., Hancock, B.C. The coefficient of restitution of some pharmaceutical tablets/compacts. *Int. J. Pharm.* **402**, 50-56 (2010).
8. Fu, J., Adams, M.J., Reynolds, G.K., Salman, A.D., Hounslowa, M.J. Impact deformation and rebound of wet granules. *Powder Technol.* **140**, 248-257 (2004).
9. Sommerfeld, M., Huber, N. Experimental analysis and modelling of particle-wall collisions. *Int. J. Multiphas. Flow.* **25**, 1457-1489 (1999).
10. Foerster, S.F., Louge, M.Y., Chang, H., Allia, K. Measurements of the collision properties of small spheres. *Phys. Fluids.* **6** (3), 1108-1115 (1994).
11. Lorenz, A., Tuozzolo, C., Louge, M.Y. Measurements of Impact Properties of Small, Nearly Spherical Particles. *Exp. Mech.* **37** (3), 292-298 (1997).
12. Fu, J., Adams, M.J., Reynolds, G.K., Salman, A.D., Hounslowa, M.J. Impact deformation and rebound of wet granules. *Powder Technol.* **140**, 248-257 (2004).
13. Wong, C.X., Daniel, M.C., Rongong, J.A. Energy dissipation prediction of particle dampers. *J. Sound Vib.* **319**, 91-118 (2009).
14. Louge, M.Y., Tuozzolo, C., Lorenz, A. On binary impacts of small liquid-filled shells. *Phys. Fluids.* **9**, 3670-3677 (1997).

